Oral Presentation

The 7th TSME International Conference on Mechanical Engineering
13-16 December 2016

TSME ICOME 2016
Mechanical Engineering Innovation for Green Society

DRC0004

Experimental observation of sideband patterns of gearboxes with different kinds of local fault

Tianyang Wang*, Fulei Chu

Department of Mechanical Engineering, Tsinghua University, Beijing 100084, China
* Corresponding Author: wty19850925@126.com, Telephone Number: 86-13581583746

Abstract

Localized gear fault is one of the most common fault types in a gear drive train. However, current studies consider all of the localized faults as one type, cannot classify different types of local fault, such as spalling, chipped, and crack faults. This will affect the precise fault diagnosis of gear drive train, which is extremely needed in a real engineer. As such, several experiments are firstly done with different kinds of local fault in this manuscript, and the traditional gear fault characteristics in both time domain and frequency domain are then calculated can compared with each other. Also, several popular algorithms, such as time synchronous average (TSA), cepstrum are finally employed to analysis the raw signal. The analysis results are listed as a conclusion which may be helpful for relative researchers.

Keywords: Fault diagnosis, Gear drivetrain, Localized fault, sidebands, TSA.

1. Introduction

Gearboxes play a crucial role in safe overall machinery operation of mechanical transmission systems. A gearbox fault may lead to unwanted shutdowns, high maintenance costs, and even human casualties. As a result, corresponding condition monitoring and fault diagnosis have long been topics of interest in both academia and industry. Regarding gear fault detection, various symptoms have been considered including vibration[1], acoustic emission[2], electrical current[3], oil debris[4], and heat[5]. Among these techniques, vibration analysis is one of the most popular methods for gear fault detection. In vibration-based gear fault diagnosis, several statistical features have been proposed to describe the fault condition[6-7].

Localized fault is one of the most common types of gear fault. It will lead to the worse incident if no effective algorithm can be proposed. However, current studies consider all of the localized faults as one type, cannot classify different types of local fault, such as spalling, chipped, and crack faults. This will affect the precise fault diagnosis of gear drive train, which is extremely needed in real engineering. According to this problem, several experimental tests are firstly carried out in this paper, and traditional algorithms in time and frequency domain are then used to analysis the measured signal in different fault types. At last, the analysis results are summarized and listed as a conclusion.

The rest of paper are structured as follows: Section 2 introduces the experimental setup, Section 3 displays the analysis results using traditional algorithms, Section 4 summarizes the experimental observations as the conclusion.

2. Experimental setup

In this paper, all of the experimental tests are performed using a gearbox test rig at Tsinghua University. Four operational modes are carried out, which are, healthy condition, spalling fault, chipped fault and crack fault. Figure 1 shows the experimental setup. A motor controlled by an alternating current (AC) inverter was used to drive the input shaft of a single-stage gearbox. A tachometer and an accelerometer were mounted on the test rig to measure the motor rotational speed and the vibration signal, respectively. A magnetic powder brake was connected to the output shaft to induce a workload.

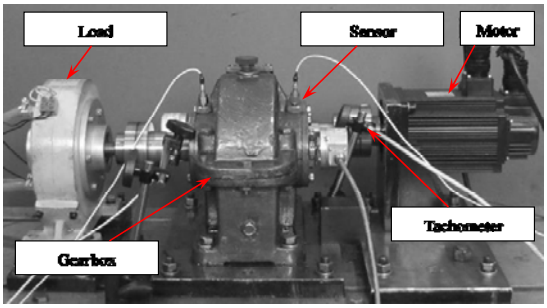

Fig. 1 Experimental set-up for gear fault detection and diagnosis

Table 2. Test gearbox parameters

Number of teeth in driving gear	Number of teeth in driven gear	Gear ratio
22	55	2.5
Module	Tooth width in driving gear	Tooth width in driven gear
1.5	2.7 cm	2.4 cm

The sampling rate was 32768 samples/s, and data were collected for 15 s. Table 1 lists the parameters of the gearbox. Localized faults were manually added to the driven gear. Figure 2(a–d) illustrates gears with different working conditions respectively.

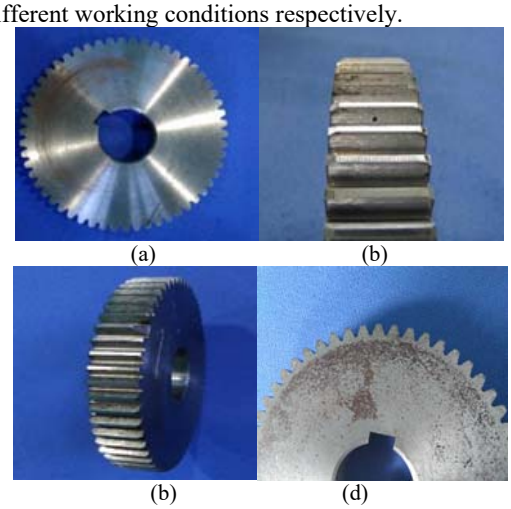

Fig. 2 Experimental test gears: (a) healthy gear, (b) spalling tooth, (c) chipped tooth, and (d) faulty gear cracks

In detail, the rotational speed of the input shaft is 1000rpm. According to the parameters listed in Table 2, the meshing frequency (f_m) is 367 Hz, the rotational frequency of the input shaft ($f_{r,i}$) is 16.67 Hz, and the rotational frequency of the faulty gear ($f_{r,o}$) is 6.67Hz.

2.1 Time domain

In this section, three widely used parameters are employed to analysis the gear meshing vibration signals under four different operating modes, which are separately kurtosis value, RMS, and FM0. Fig. 3 ~ Fig. 5 give the parameters' values under different operating modes.

1. kurtosis

Kurtosis is the fourth normalized moment of a given signal x and provides a measure of peakness of the signal. In this way, the kurtosis value is an important parameter to indicate the localized fault. The corresponding equations are shown as follow:

$$kurtosis = \frac{N\sum_{i=1}^{N}(x_i-\bar{x})^4}{[\sum_{i=1}^{N}(x_i-\bar{x})^2]^2} \quad (1)$$

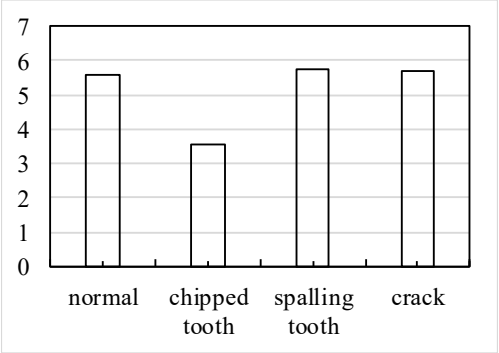

Fig. 3 kurtosis values under different operating conditions

2. Root mean squared (RMS)

Root mean squared (RMS) is defined as the square root of the average of the sum of the squares of the measured signal. Eq. (2) gives the specific equation as follow:

$$RMS_x = \sqrt{\frac{1}{N}[\sum_{i=1}^{N}(x_i)^2]} \quad (2)$$

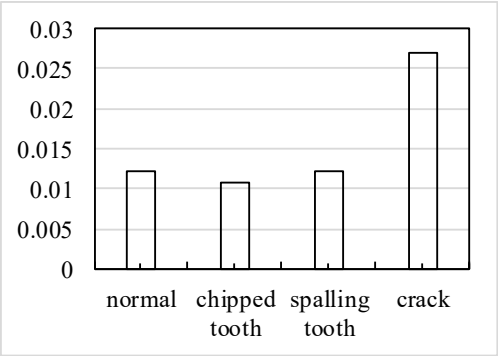

Fig. 4 RMS under different operating conditions

3. FM0

The parameter FM0 was proposed in [8] as a robust indicator of major faults in a gear mesh. FM0 is the ratio between the maximum peak-to-peak amplitude of the signal x and the sum of the amplitudes of the meshing frequency and its harmonics as expressed by Eq. (3).

$$FM0 = \frac{PP_x}{\sum_{n=0}^{H} P_n} \quad (3)$$

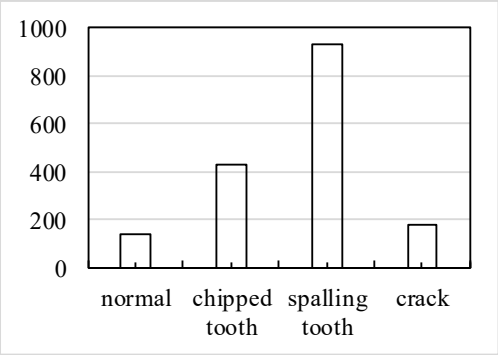

Fig. 5 FM0 under different operating conditions

Based on Fig. 3 ~ Fig. 5, three conclusions can be summarized:

(1) Kurtosis value is suitable to detect chipped tooth fault.
(2) RMS value is suitable for identifying the tooth crack.
(3) FM0 can be used to detect the faults of the spalling tooth.

2.2 Frequency domain

In this section, the raw spectrums of gear meshing signal under different working conditions are calculated and displayed in Fig. 6 ~ Fig. 9, respectively.

DRC0004

In the healthy condition, prominent peaks at meshing frequency, its harmonics, and the sidebands around them spacing at $f_{r,i}$ and $f_{r,o}$ can be located. In this sense, just identifying the sidebands cannot indicate a fault condition.

If there exists localized fault on the driven gear, following three different observations can be summarized:

(1) The meshing frequency is more prominent under chipped tooth and crack faults than the one under the healthy condition.
(2) Under faulty conditions, the magnitudes of the sidebands spacing at the $f_{r,i}$ (the gear mounted on the input shaft is health) are relatively lower.
(3) It's not easy to identify the spalling tooth fault just based on the raw spectrum.

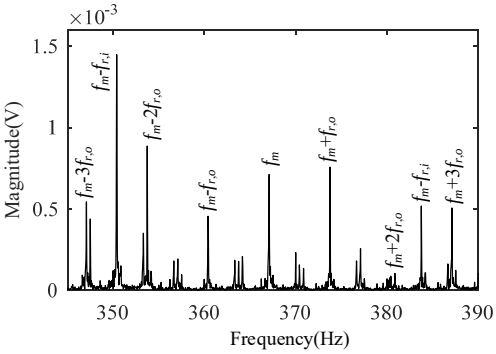

Fig. 6 Spectrum of a healthy gear meshing signal

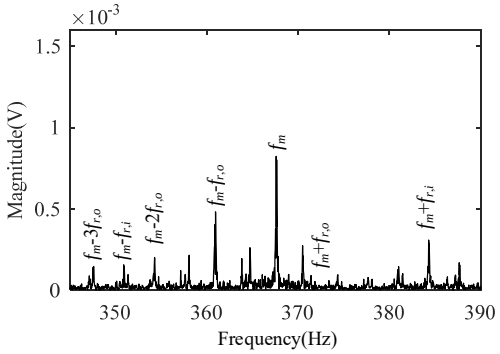

Fig. 7 Spectrum of a gear meshing signal with a chipped tooth fault

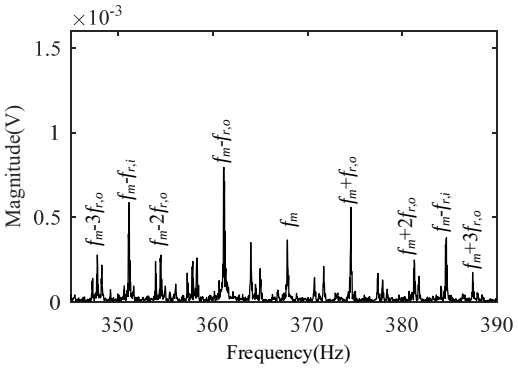

Fig. 8 Spectrum of a gear meshing signal with a spalling tooth fault

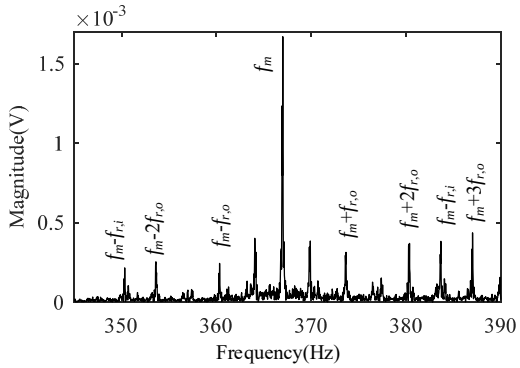

Fig. 9 Spectrum of a gear meshing signal with a crack fault

If there exists localized fault on the driven gear, following three different observations can be summarized:

(4) The meshing frequency is more prominent under chipped tooth and crack faults than the one under the healthy condition.
(5) Under faulty conditions, the magnitudes of the sidebands spacing at the $f_{r,i}$ (the gear mounted on the input shaft is health) are relatively lower.
(6) It's not easy to identify the spalling tooth fault just based on the raw spectrum.

2.3 Time synchronous average (TSA)

In this section, the TSA algorithm is used to analysis the vibration signal at first, and then the fast Fourier transform (FFT) is used to obtain the spectrums of the average results. Fig. 10 ~ Fig. 13 present the corresponding TSA algorithm based spectrums.

In the healthy condition shown in Fig. 10, the peaks representing meshing frequency (f_m) and its second harmonics ($2f_m$) can be located. Around the meshing frequency, two sidebands spacing at $3f_{r,o}$ and $5f_{r,o}$ can be located, and the sidebands spacing at $2f_{r,o}$ can be found around the $2f_m$.

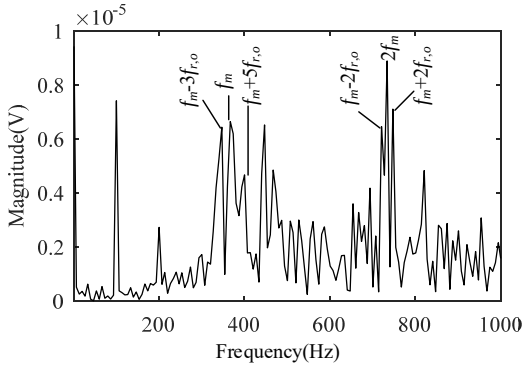

Fig. 10 TSA based spectrum of a healthy gear meshing signal

Comparing to the healthy condition, the TSA based spectrums under fault conditions have following characteristics:

(a) The meshing frequency in all of the faulty conditions is more prominent than the one of the healthy condition.

(b) As for the status of spalling fault, the second harmonic of the meshing frequency is extremely low.
(c) As for the situations of spalling fault and crack fault, more sidebands around the meshing frequency and its harmonics can be found.

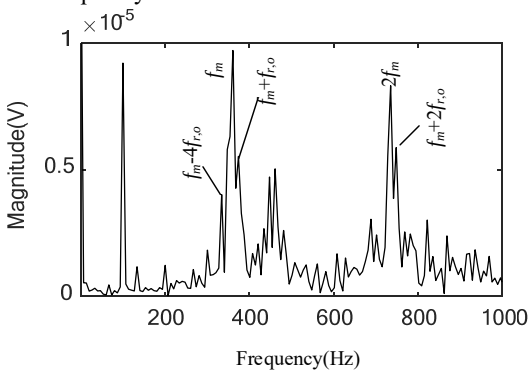

Fig. 11 TSA based spectrum of a gear meshing signal with a chipped tooth fault

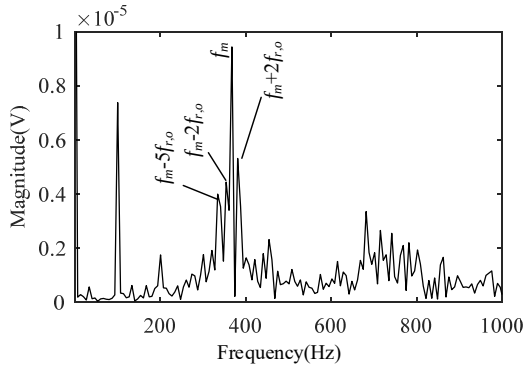

Fig. 12 TSA based Spectrum of a gear meshing signal with a spalling tooth fault

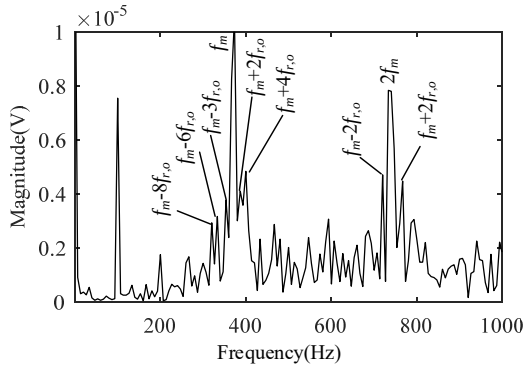

Fig. 13 TSA based spectrum of a gear meshing signal with a spalling tooth fault

2.4 Cepstrum

In this section, the cepsturms of the vibration signals under different working conditions are calculated and displayed in Fig. 14 ~ Fig. 17. In Fig. 14, the peaks representing the rotational frequencies of input and output shafts can be easily located. In detail, the input shaft rotational frequency ($f_{r,i}$) and its harmonics are pointed by black arrows and the output shaft rotational frequency ($f_{r,o}$) and its harmonics are pointed by red arrows.

Fig. 15 ~ Fig. 17 shows the corresponding cepstrums under different working conditions of spalling fault, chipped fault and crack fault. According to these cepstrums, following two conclusions can be drawn.

(a) Under the conditions of chipped and spalling tooth fault, the peaks representing input shaft rotational frequency and its harmonics have relatively lower magnitudes. This phenomenon can indicate that cepstrum based algorithm is more suitable for these two kinds of faults.
(b) The cepstrums of healthy signal and the one with crack fault are similar to each other, which means that the cepsturm method cannot detect the crack fault.

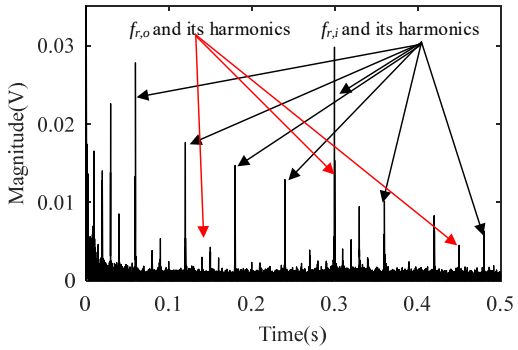

Fig. 14 Cepstrum of a healthy gear meshing signal

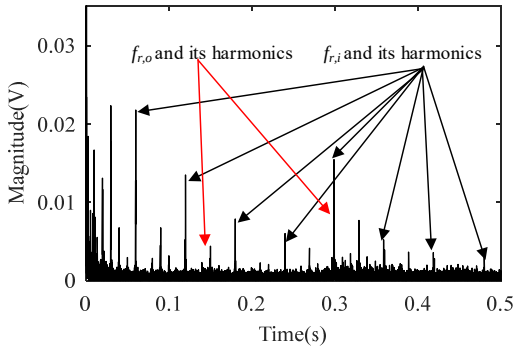

Fig. 15 Cepstrum of a gear meshing signal with a chipped tooth fault

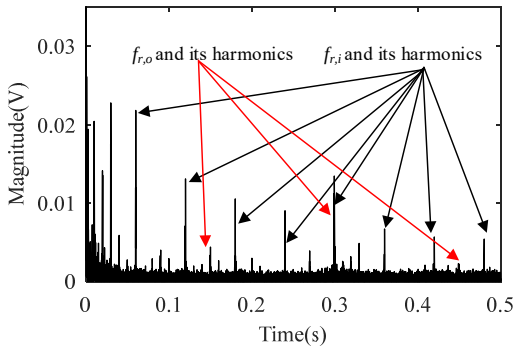

Fig. 16 Cepstrum of a gear meshing signal with a spalling tooth fault

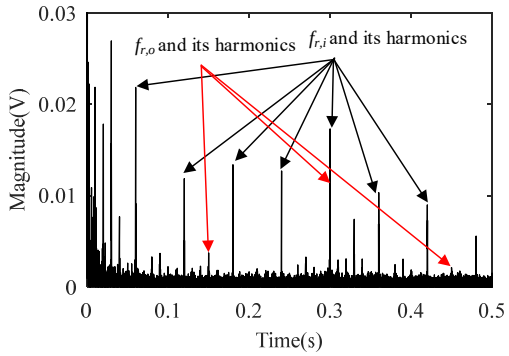

Fig. 17 Cepstrum of a gear meshing signal with a crack fault

4. Conclusion

In this paper, four basic methods, which are time-domain parameters, raw spectrum, TSA-based spectrum analysis, and cepstrum, are used to analysis gear meshing signals under four different working conditions. Several observations can be summarized:

(1) If no fault is presented on the monitored gearbox, the magnitudes of all of the parameters are relatively low. And the magnitudes of the peaks representing the meshing frequency and its harmonics are not higher than the ones representing the sidebands. No unique feature can be found in the corresponding TSA based spectrum and cepstrum.

(2) As for the chipped fault, the kurtosis value of the vibration signal becomes lower than one of the healthy condition and other fault types. In the raw spectrum and the TSA based spectrum, the magnitude of the meshing frequency become prominent. And no obviously characteristic can be found in the corresponding cepstrum.

(3) If a spalling fault happens, the FM0 value increases obviously. In the raw spectrum, the meshing frequency is not prominent as the situations of other fault conditions. And in the TSA based spectrum, the meshing frequency become prominent. However, its second harmonic become relatively low.

(4) When a tooth crack appears, the RMS value increases sensitively. The sidebands around the meshing frequency in the TSA based spectrum is much richer than the ones under other fault types.

5. Acknowledgement

The research work described in this paper was supported by Natural Science Foundation of China under Grant No. 51335006 and No. 51605244.

6. References

[1]. Lei, Y., Li, N., Lin, J., & He, Z. (2013). Two new features for condition monitoring and fault diagnosis of planetary gearboxes. *Journal of Vibration and Control*, vol. 0(0), 2013,pp. 1-10.

[2]. Tan, C. K., & Mba, D. (2005). Identification of the acoustic emission source during a comparative study on diagnosis of a spur gearbox. *Tribology International*, vol. 38(5), 2005,pp. 469-480.

[3]. A., R. M., & C., K. (2006). Fault Detection in a Multistage Gearbox by Demodulation of Motor Current Waveform. *IEEE Transactions on Industrial Electronics*, vol. 53(4), 2006,pp. 1285-1297.

[4]. Peng, Z., & Kessissoglou, N. (2003). An integrated approach to fault diagnosis of machinery using wear debris and vibration analysis. *Wear*, vol. 255(7 – 12), 2003,pp. 1221-1232.

[5]. Younus, A. M. D., & Yang, B. (2012). Intelligent fault diagnosis of rotating machinery using infrared thermal image. *Expert Systems with Applications*, vol. 39(2), 2012,pp. 2082-2091.

[6].Ma, J. (1995, 1995-01-01). *Energy operator and other demodulation approaches to gear defect detection*.

[7]. Saravanan, N., Siddabattuni, V. N. S. K., & Ramachandran, K. I. (2008). A comparative study on classification of features by SVM and PSVM extracted using Morlet wavelet for fault diagnosis of spur bevel gear box. *Expert Systems with Applications*, vol. 35(3), 2008,pp. 1351-1366.

[8].Stewart, R. M. (1977). *Some useful data analysis techniques for gearbox diagnostics*: University of Southampton.